Supporting Materials:
Performance of prominent torque control methods for tethered lower-limb exoskeletons during human walking

Juanjuan Zhang, Chien Chern Cheah, Steven H. Collins,

1 Sequence of experimental conditions

Experiments were conducted over the course of 3 days, with all data for each high-level assistance controller collected on the same day. Low-level torque controllers were collected in the same order for each high-level controller, except for a change in the order of the PAS controller for the Time-based desired torque (which was accidentally skipped, then caught at the end of the collection). The exact sequence is shown in Table S1.

Sequence	Day 1 Afternoon	Day 2 Morning	Day 2 Afternoon	Day 3 Afternoon
	TIME	NMM	ANGLE	EMG
↓	PD*	PD*	PD*	PD*
	PD*+M	PD*+M	PD*+M	PD*+M
	PID*	PID*	PID*	PID*
	PD*+EDG	PD*+EDG	PD*+EDG	PD*+EDG
↓	PD*+PEC	PD*+PEC	PE+PEC	PD*+PEC
	LRN	PAS	PAS	PAS
	LRN+PD*	LRN	LRN	LRN
↓	PD*+ΔLRN	LRN+PD*	LRN+PD*	LRN+PD*
	PAS	PR+LRN	PD*+ΔLRN	PD*+ΔLRN

Table SI: Data collection timeline

2 Ankle Angle versus Time

Fig. S1 shows trajectories of exoskeleton ankle joint angles in time for 100 strides, and a time-averaged trajectory, for each combination of high- and low-level controller. With Ankle-based and NMM-based desired torque, trajectories were similar to those of the biological ankle joint during normal human walking. With Time-based and EMG-based desired torque, less ankle excursion occurred on an average step. Variability in joint angle was highest when desired torque was based on Time.

3 Torque versus Ankle Angle

Fig. S2 shows ankle torque versus ankle angle for 100 strides, and the time-averaged torque versus time-averaged joint angle, for each combination of high- and low-level controller. With Ankle-based and NMM-based desired torque, trajectories were similar to those of the biological ankle joint during normal human walking. With EMG-based desired torque, torque-angle curves have consistent shape across torque controllers, characterized by very steep slopes in angle space with approximately infinite impedance in places. With Time-based desired torque, torque-angle curves were complex and nonlinear. Changes in torque-angle relationships across low-level torque controllers within the same high-level controller (within the same column)

suggest either interactions between torque control mode and human coordination pattern, or subject adaptations over time. Curves tend to move in a clockwise direction, indicating positive work production by the exoskeleton.

Fig. S3 shows the ankle torque versus ankle angle curve for 100 strides, and the time-averaged torque versus time-averaged joint angle, for the case when motor position was held constant. This passive relationship between joint angle and joint torque seemed to be related to the difficulty of tracking desired torques generated by different high-level controllers; desired curves that were closer to the passive curve seemed easier for, e.g., PD* control, while LRN control made larger improvements when the two curves were dissimilar.

4 T-Test Results for Controller RMS-E Values

Table SII-SV shows the t-test mean comparison p value of every two low level torque controllers within each high level controller. We used a significance level of α=0.05. P-values that are beyond the threshold are shown in red. Almost all comparisons were highly statistically significant. Please see main text for effect size information.

	PD*	PD*+EDG	PD*+PEC	PID*	PD*+M	PAS	LRN	LRN+PD*
PD*+EDG	1.1e-22	·	·	·	·	·	·	·
PD*+PEC	1.4e-20	4.2e-42	·	·	·	·	·	·
PID*	6.1e-34	1.5e-52	2.9e-08	·	·	·	·	·
PD*+M	2.1e-169	4.2e-140	1.2e-174	4.0e-182	·	·	·	·
PAS	1.3e-06	3.5e-32	2.8e-05	7.5e-17	1.1e-175	·	·	·
LRN	1.9e-94	7.1e-113	1.0e-84	8.9e-81	4.6e-178	6.1e-93	·	·
LRN+PD*	6.3e-153	2.1e-107	2.7e-144	5.2e-114	7.9e-182	7.5e-126	3.7e-08	·
PD*+ΔLRN	8.4e-157	9.8e-110	8.0e-149	2.7e-118	1.1e-182	1.7e-129	1.5e-15	5.6e-10

Table SII: Time-based desired torque RMS-E t-test p values.

	PD*	PD*+EDG	PD*+PEC	PID*	PD*+M	PAS	LRN	LRN+PD*
PD*+EDG	4.3e-143	·	·	·	·	·	·	·
PD*+PEC	9.3e-01	5.0e-145	·	·	·	·	·	·
PID*	1.3e-06	7.2e-151	6.1e-07	·	·	·	·	·
PD*+M	3.4e-164	6.7e-130	2.8e-162	6.1e-164	·	·	·	·
PAS	4.1e-01	1.3e-129	4.5e-01	1.8e-07	6.1e-173	·	·	·
LRN	8.3e-06	7.5e-15	8.8e-06	1.2e-07	2.6e-60	1.8e-05	·	·
LRN+PD*	7.2e-58	7.0e-130	4.9e-58	1.0e-48	4.3e-195	1.0e-58	2.8e-19	·
PD*+ΔLRN	1.5e-52	4.1e-130	8.4e-53	1.1e-42	1.4e-193	4.1e-53	1.1e-17	2.1e-02

Table SIII: Angle-based desired torque RMS-E t-test p values.

5 Convergence Time for Controllers with Iterative Learning Components

Fig. S4 shows convergence of RMS-E and RMS-E AVG tracking errors over time for the three torque controllers that involved iterative learning. Each dot denotes the RMS-E or RMS-E AVG for a 20-step period starting from the stride number on the x-axis. Solid lines are the exponential fits to the error trends. Convergence was slowest and the reduction in error greatest when desired torque was based on Time. Improvements were more modest with Angle- and NMM-based desired torque. When desired torque was based on EMG, learning resulted in large initial improvements in torque error, but high errors remained at steady state.

	PD*	PD*+EDG	PD*+PEC	PID*	PD*+M	PAS	LRN	LRN+PD*
PD*+EDG	4.4e-113	·	·	·	·	·	·	·
PD*+PEC	3.0e-11	1.1e-86	·	·	·	·	·	·
PID*	3.2e-08	3.2e-104	2.5e-02	·	·	·	·	·
PD*+M	1.3e-238	3.1e-175	6.3e-172	2.5e-213	·	·	·	·
PAS	1.2e-11	9.3e-85	8.1e-01	1.4e-02	8.3e-169	·	·	·
LRN	7.5e-38	7.1e-91	5.7e-49	4.2e-45	9.4e-131	2.3e-49	·	·
LRN+PD*	2.6e-119	1.3e-166	1.4e-104	2.1e-121	1.6e-241	4.1e-103	4.1e-19	·
PD*+ΔLRN	8.2e-72	1.5e-133	8.9e-84	1.2e-81	3.0e-174	1.0e-83	8.4e-07	1.3e-09

Table SIV: NMM-based desired torque RMS-E t-test p values.

	PD*	PD*+EDG	PD*+PEC	PID*	PD*+M	PAS	LRN	LRN+PD*
PD*+EDG	1.9e-41	·	·	·	·	·	·	·
PD*+PEC	9.9e-15	4.5e-20	·	·	·	·	·	·
PID*	1.7e-01	3.0e-41	1.4e-12	·	·	·	·	·
PD*+M	6.9e-52	1.4e-06	1.2e-32	2.2e-51	·	·	·	·
PAS	1.4e-10	1.5e-26	4.5e-02	2.5e-08	1.9e-38	·	·	·
LRN	3.1e-04	3.8e-10	2.5e-01	3.6e-03	4.0e-17	9.1e-01	·	·
LRN+PD*	7.5e-37	1.0e-87	4.0e-67	3.8e-45	4.6e-91	1.5e-63	1.5e-26	·
PD*+ΔLRN	1.9e-34	2.7e-84	2.5e-63	4.8e-42	5.2e-89	1.5e-59	7.8e-26	6.8e-01

Table SV: EMG-based desired torque RMS-E t-test p values.

6 Relative contributions of the desired motor displacements of various components of PD*+ΔLRN for all four high level controllers

Fig. S5 shows convergence of RMS-E and RMS-E AVG tracking errors over time for the three torque controllers that involved iterative learning. Each dot denotes the RMS-E or RMS-E AVG for a 20-step period starting from the stride number on the x-axis. Solid lines are the exponential fits to the error trends. Convergence was slowest and the reduction in error greatest when desired torque was based on Time. Improvements were more modest with Angle- and NMM-based desired torque. When desired torque was based on EMG, learning resulted in large initial improvements in torque error, but high errors remained at steady state.
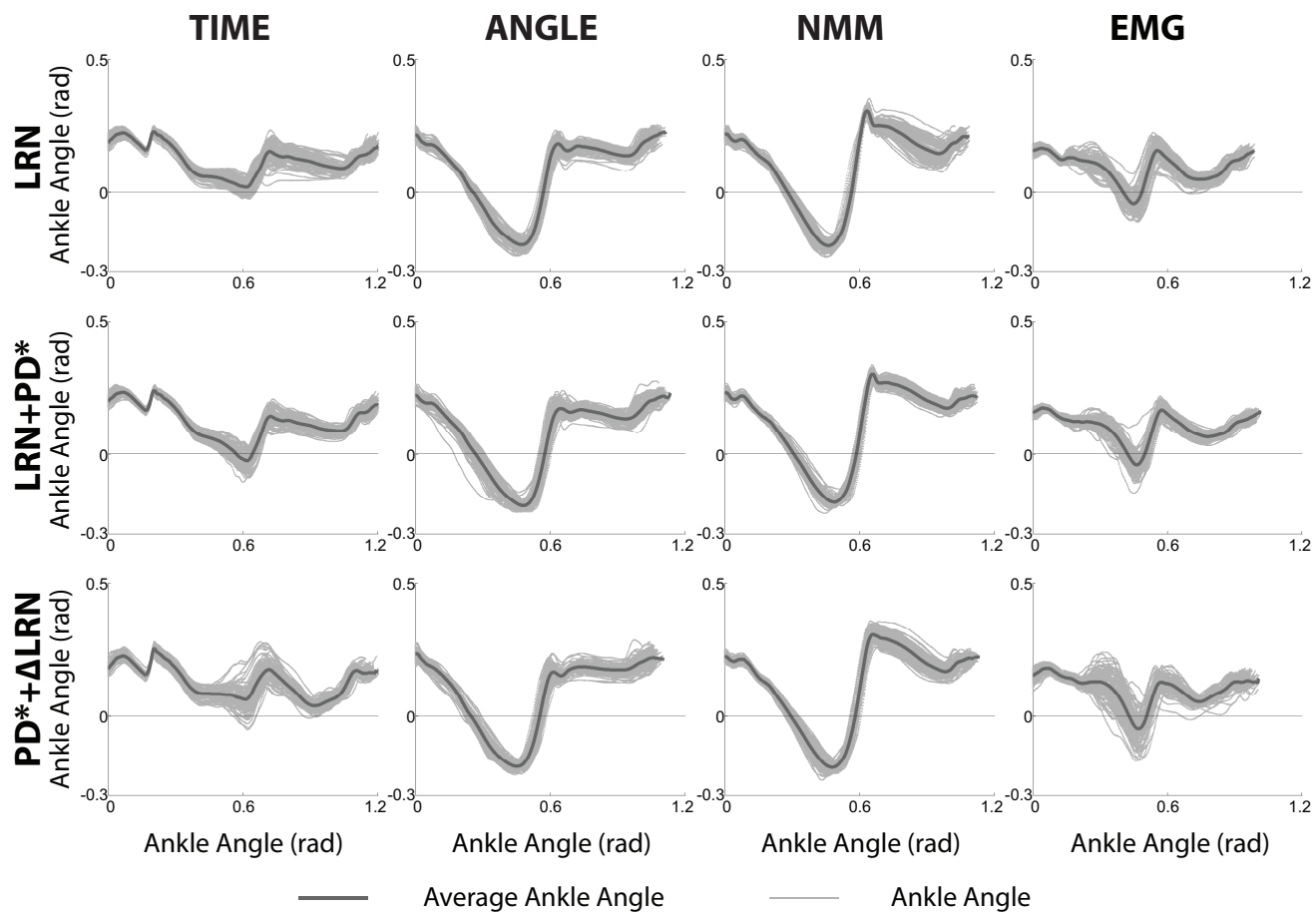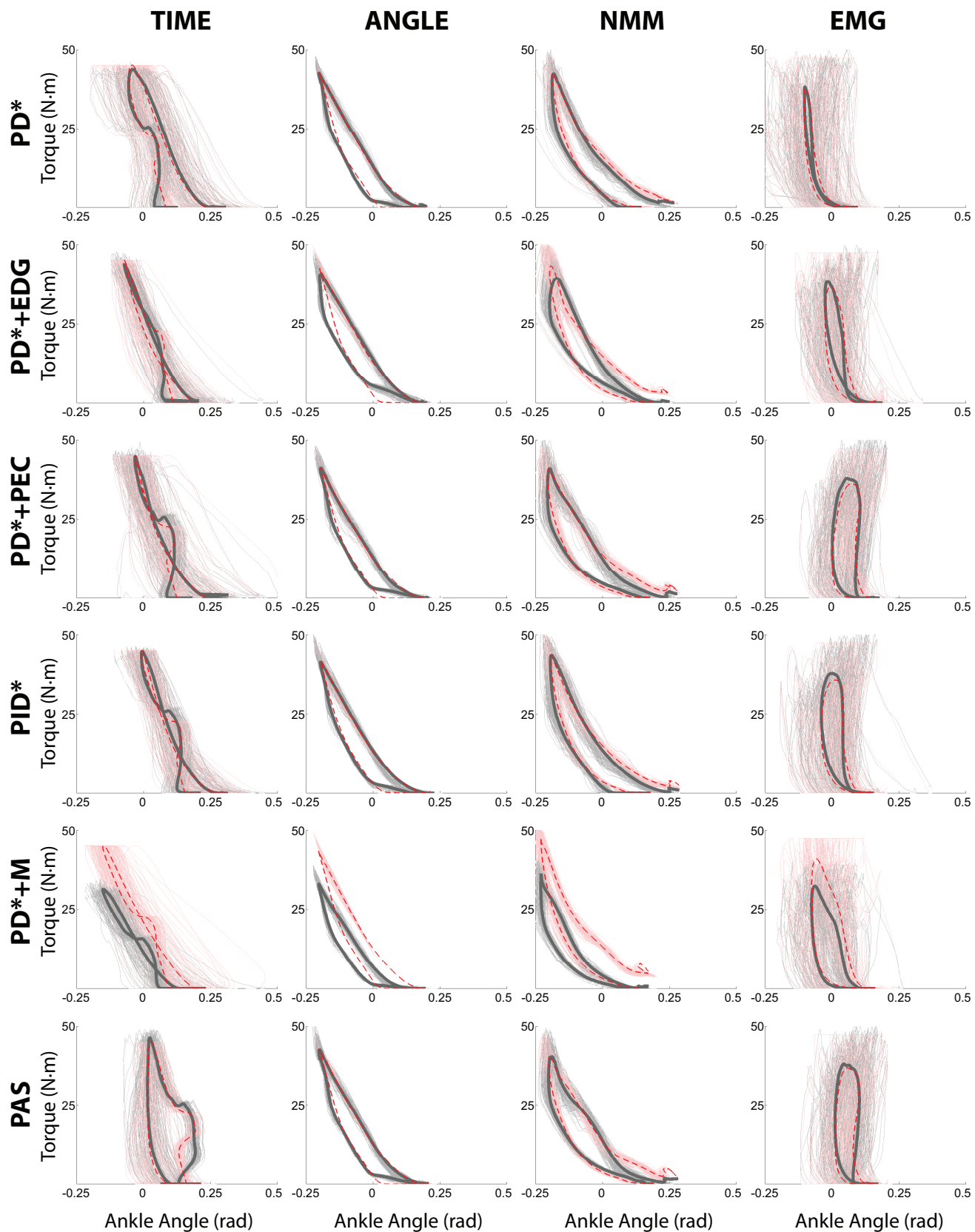
TIME   ANGLE   NMM   EMG

PD*

PD*+EDG

PD*+PEC

PID*

PD*+M

PAS

Ankle Angle (rad)

4
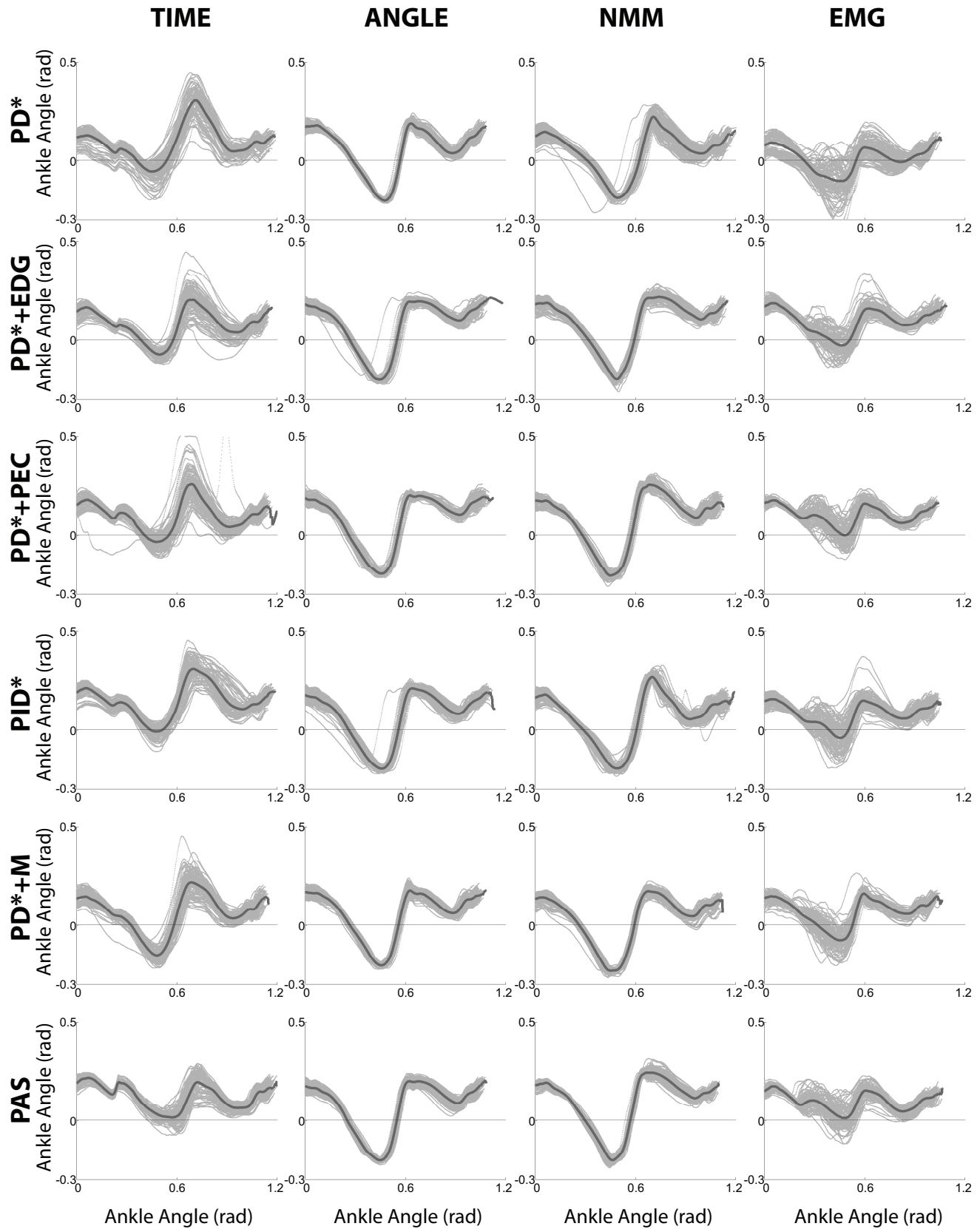
Fig. S1: Overlapped trajectories of measured ankle angle in time for 100 steady-state strides.

Figure columns: **TIME**, **ANGLE**, **NMM**, **EMG**

Figure rows: **PD***, **PD*+EDG**, **PD*+PEC**, **PID***, **PD*+M**, **PAS**

y-axis label: Torque (N·m)

x-axis label: Ankle Angle (rad)
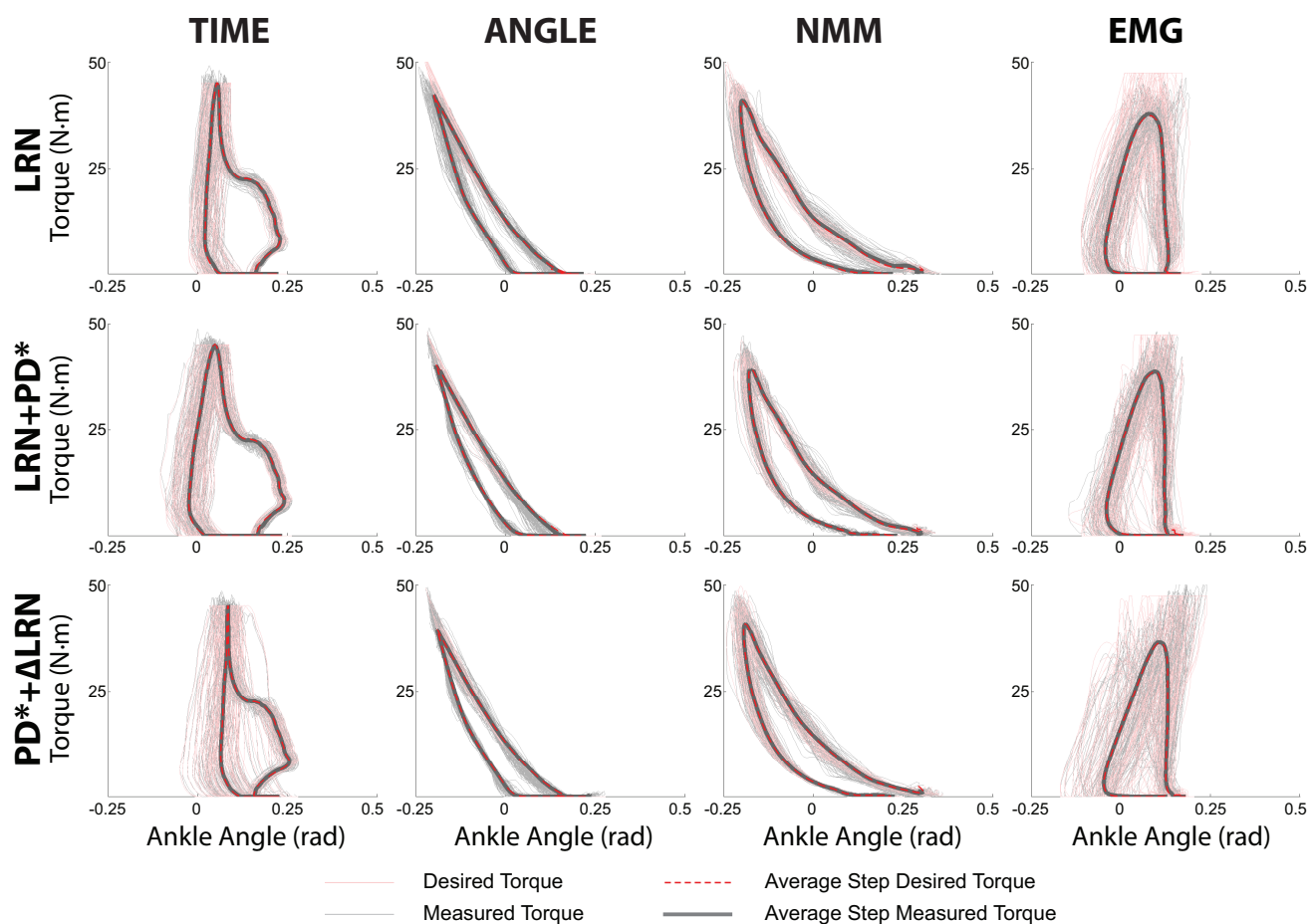
Fig. S2: Overlapped trajectories of measured ankle torque versus measured ankle angle for 100 steady-state strides.
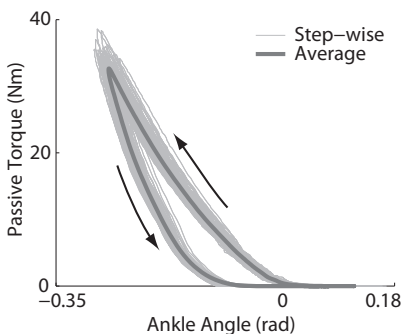
Fig. S3: Passive response: overlapped trajectories of measured ankle torque versus measured ankle angle for 100 strides during which the motor position was fixed.).
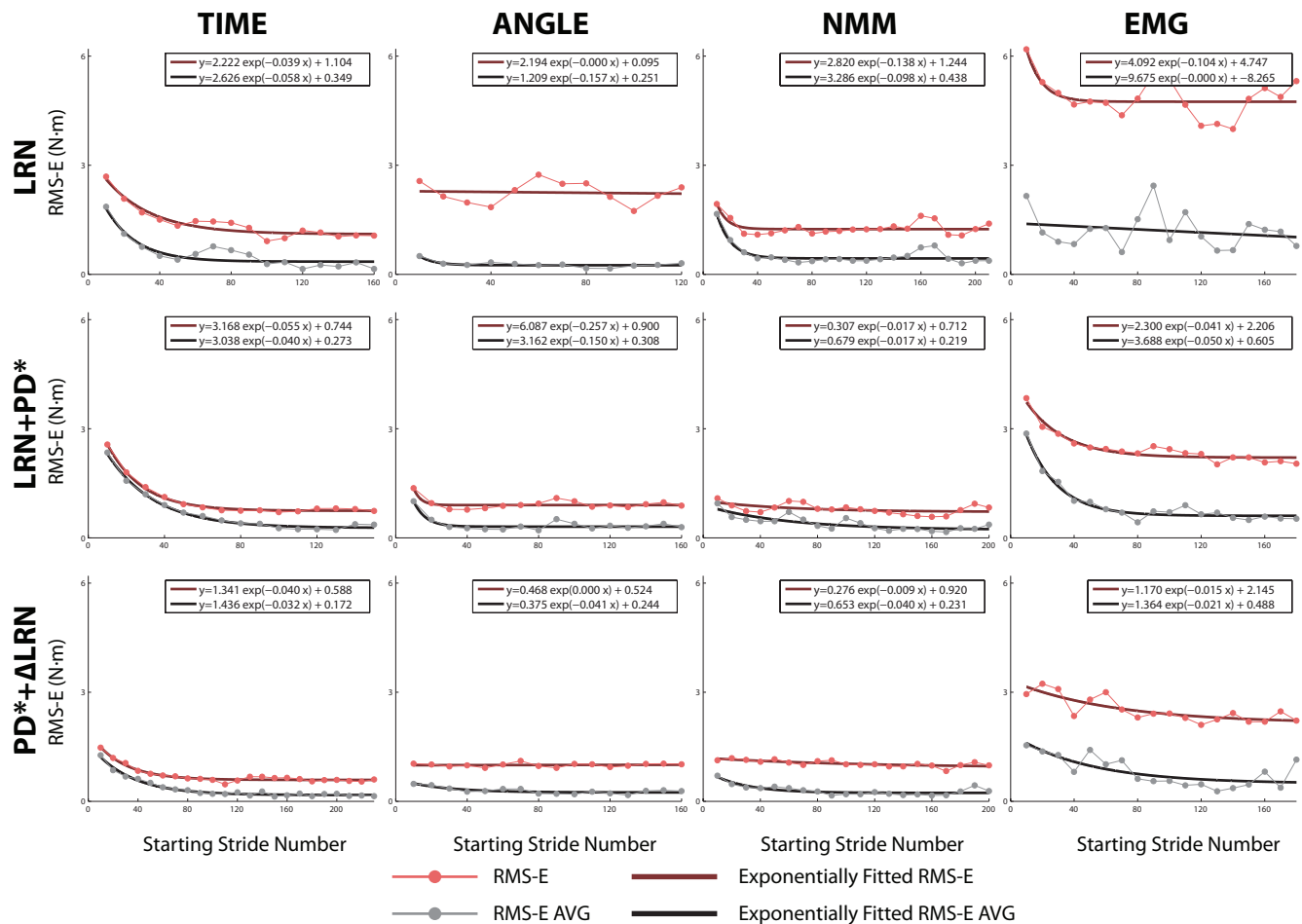
Fig. S4: Error as a function of time for controllers with iterative learning components. Each dot is the average RMS error for 20 strides, beginning with the number indicated on the x axis.
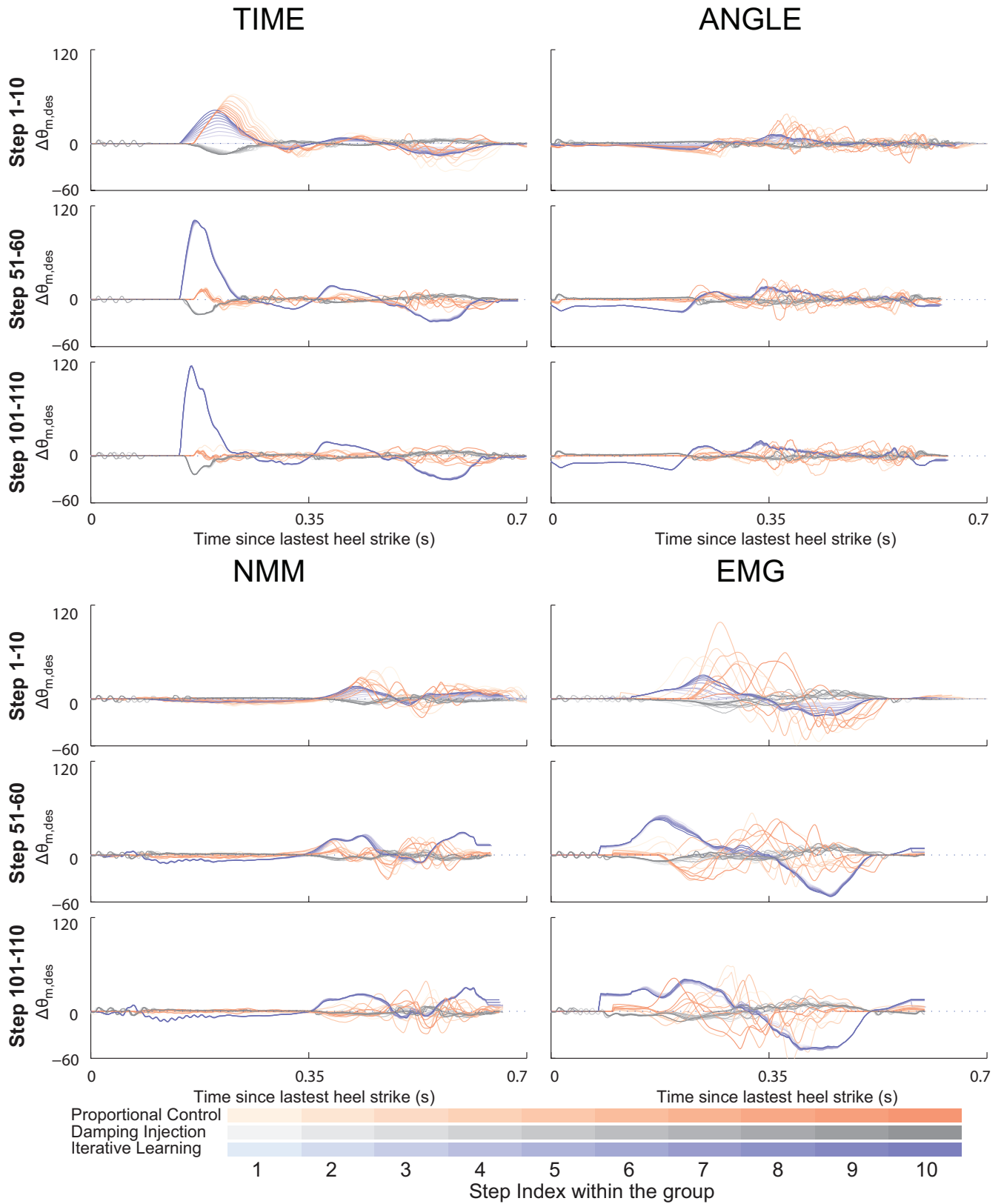
Fig. S5: Contributions from various elements towards the control input, the desired motor displacements, of PD*+ΔLRN controller for four different high level controllers.